

# A Novel Disulfide Pattern in Laminin-Type Epidermal Growth Factor-like (LE) Modules of Laminin $\beta$ 1 and $\gamma$ 1 Chains<sup>†</sup>

Stefan Kalkhof,<sup>‡,△,¶</sup> Konstanze Witte,<sup>‡,¶</sup> Christian H. Ihling,<sup>‡</sup> Mathias Q. Müller,<sup>‡</sup> Manuel V. Keller,<sup>§,||</sup> Sebastian Haehn,<sup>§</sup> Neil Smyth,<sup>⊥</sup> Mats Paulsson,<sup>§,||</sup> and Andrea Sinz<sup>\*,‡</sup>

<sup>‡</sup>Department of Pharmaceutical Chemistry and Bioanalytics, Institute of Pharmacy, Martin Luther University Halle-Wittenberg, D-06120 Halle (Saale), Germany, <sup>§</sup>Center for Biochemistry and Center for Molecular Medicine, Faculty of Medicine, University of Cologne, D-50931 Cologne, Germany, <sup>||</sup>Cologne Excellence Cluster on Cellular Stress Responses in Aging Associated Diseases (CECAD), D-50931 Cologne, Germany, and <sup>⊥</sup>School of Biological Sciences, University of Southampton, East Southampton SO16 7PX, United Kingdom <sup>△</sup>Present address: Department of Proteomics, Helmholtz Center for Environmental Research—UFZ, D-04318 Leipzig, Germany <sup>¶</sup>Both authors contributed equally to this work

Received July 27, 2010; Revised Manuscript Received August 18, 2010

**ABSTRACT:** *In-depth* mass spectrometric analysis of disulfide bond patterns in recombinant mouse laminin  $\beta$ 1 and  $\gamma$ 1 chain N-terminal fragments comprising the laminin N-terminal (LN) domain and the first four laminin epidermal growth factor-like (LE) domains revealed a novel disulfide pattern for LE domains. This showed a (2–3, 4–5, 6–7, 8–1) connectivity with the last cysteine of one LE domain being connected to the first cysteine of the following LE domain. The same pattern was also found in E4, the N-terminal  $\beta$ 1 chain fragment derived by elastase digestion of mouse EHS tumor laminin-111, showing that this pattern occurs in native laminin. The strictly linear pattern with an interdomain disulfide has not been described previously for EGF domains. The N-terminal portions of laminin short arms, consisting of the LN domain and LE domains 1–4, are essential for laminin–laminin self-interactions, whereas the internal LE domains 7–9 in the laminin  $\gamma$ 1 chain harbor the nidogen binding site and have a conventional disulfide pattern. This suggests that LE domains differing in function also differ in their disulfide patterns.

Epidermal growth factor (EGF)<sup>1</sup> domains are extracellular protein modules, which are cross-linked by intramolecular disulfide bonds. Structurally, the classical EGF domain is described as a small domain of 30–40 amino acids primarily stabilized by three disulfides with the connectivity (1–3, 2–4, 5–6) (1). Two different types of three-disulfide EGF domains can be differentiated on the basis of the structure of the C-terminal half of the last disulfide loop (2). In addition to these three-disulfide EGFs, structures of three four-disulfide EGF domains, derived from the laminin  $\gamma$ 1 chain and integrin  $\beta$ 2 and  $\beta$ 3 subunits, have been solved (3–5). These four-disulfide EGF domains possess an additional intradomain disulfide showing a (1–3, 2–4, 5–6, 7–8) connectivity called “laminin-type EGF-like domain” or a

(1–5, 2–4, 3–6, 7–8) connectivity termed “integrin-type EGF-like domain”.

Laminins are the major noncollagenous proteins within the basement membrane and are crucial for its formation. Laminin short arms are formed by the C-terminal portions of laminin chains and are required for laminin polymerization. They consist of two ( $\beta$  and  $\gamma$ ) or three ( $\alpha$ ) globular domains interspersed by series of laminin-type EGF-like (LE, for nomenclature see refs 6 and 7) modules. The N-terminal (LN) globular domains are not self-folding entities but require the following four LE domains for efficient expression (8). This region of the molecule is involved in laminin polymerization and binds to the corresponding domain upon other laminin chains (9). It has also been implicated as harboring a binding site for integrin  $\alpha$ 3 $\beta$ 1 on the laminin  $\alpha$ 5 chain (10).

LE domains were originally classified as a variant of EGF modules (11, 12). Each LE domain is comprised of 50–60 amino acids, and the module was initially identified in  $\alpha$ 1,  $\beta$ 1, and  $\gamma$ 1 chains of laminin (11–13). LE modules are shared by all other laminin chain isoforms, where they occur in tandem arrays (14, 15), and by the basement membrane proteoglycans perlecan (16) and agrin (17). Series of LE domains also occur along with LN domains in netrins (18) and usherin (19), both being basement membrane associated proteins. The LE domain 8 in the laminin  $\gamma$ 1 chain provides the high-affinity binding site for nidogen-1 (20), and it has been proposed that laminin LE domains may carry growth factor activity (21).

Here we report the *in-depth* mass spectrometric analysis of the disulfide bond pattern in recombinant mouse laminin  $\beta$ 1 and  $\gamma$ 1

<sup>†</sup>This work was funded by grants SI 867/7-1 and SM 65/1-3 from the DFG (Deutsche Forschungsgemeinschaft). S.K. acknowledges support by the International Postgraduate Programme (IPP) at the University of Leipzig and the DFG-funded Graduiertenkolleg 1026 “Conformational Transitions in Macromolecular Interactions” at the Martin Luther University Halle-Wittenberg.

\*Address correspondence to this author. Tel: +49-345-5525170. Fax: +49-345-5527026. E-mail: andrea.sinz@pharmazie.uni-halle.de.

Abbreviations: CID, collision-induced dissociation; DTT, dithiothreitol; EGF, epidermal growth factor; EHS, Engelbreth–Holm–Swarm; ESI-FTICR-MS, electrospray ionization Fourier transform ion cyclotron resonance mass spectrometry; HCCA,  $\alpha$ -cyano-4-hydroxycinnamic acid; HCD, higher-energy collision-induced dissociation; HPLC, high-performance liquid chromatography; LE domain, laminin epidermal growth factor-like domain; LID, laser-induced dissociation; LN domain, laminin N-terminal domain (domain VI); LTQ, linear ion trap (ThermoFisher Scientific); MALDI-TOF-MS, matrix-assisted laser desorption/ionization time-of-flight mass spectrometry; PMF, peptide mass fingerprint; PFF, peptide fragment fingerprint; TGF, transforming growth factor.

chain fragments consisting of one LN domain and the following LE domains 1–4. The analysis of the disulfide pattern in laminin LN domains has been described by us recently (22). In the present report, disulfide patterns of the four N-terminal laminin LE domains were elucidated pointing to a novel (2–3, 4–5, 6–7, 8–1) connectivity with the last cysteine of LE domain being connected to the first cysteine in the following LE domain. This novel pattern with an interdomain disulfide bond has not been earlier described for EGF domains and sheds new light into the structure–function relationship of laminin LE domains.

## MATERIALS AND METHODS

**Reagents.** Iodoacetamide (Sigma, Taufkirchen, Germany), GdnHCl, DTT (Roth, Karlsruhe, Germany), urea (Merck, Darmstadt, Germany), and acetone were obtained at the highest available purity. The proteases trypsin, chymotrypsin, LysC, endoproteinase AspN, and GluC (all sequencing grade) were obtained from Roche Diagnostics (Mannheim, Germany); LysN was obtained from U-Protein Express BV (Utrecht, The Netherlands). MALDI matrices and peptides for MALDI-TOF-MS calibration were purchased from Bruker Daltonik (Bremen, Germany). Pepsin (3260 units/mg) as well as all other chemicals was purchased from Sigma (Taufkirchen, Germany). Nano-HPLC solvents were of spectroscopic grade (Uvasol, VWR, Darmstadt, Germany). Water was purified with a Direct-Q5 water purification system (Millipore, Eschborn, Germany).

**Protein Expression and Purification.** Expression of the recombinant mouse laminin  $\beta 1$  and  $\gamma 1$  chain fragments in human embryonic kidney 293 cells and purification from serum-free cell culture supernatant were performed as earlier described (8). Laminin-111 was isolated from mouse EHS tumor tissue and purified as described (23). Fragment E4 was a kind gift of Dr. Takako Sasaki (Shriners Hospitals for Children, Portland), having been generated from laminin-111 by digestion with bovine pancreatic elastase and chromatographically purified (24).

**Sequence Analysis.** Preliminary studies included peptide mapping to confirm the identity of the laminin fragments. For this purpose, laminin samples were fully reduced with 15 mM DTT (30 min at 56 °C), alkylated with 15 mM iodoacetamide in the presence of urea (30 min, room temperature in the dark), and digested with either trypsin, endoproteinase AspN, chymotrypsin, GluC, or a mixture of trypsin and endoproteinase AspN (1:50 (w/w) enzyme to substrate ratio) according to existing protocols (25). The resulting digests were fractionated by nano-HPLC prior to matrix-assisted laser desorption/ionization time-of-flight/time-of-flight (MALDI-TOF/TOF), nanoelectrospray ionization Fourier transform ion cyclotron resonance (ESI-FTICR), and LTQ (linear ion trap)-Orbitrap mass spectrometry.

**Disulfide Analysis.** Two strategies were applied for disulfide assignment: The first approach is based on a complete alkylation of the proteins with iodoacetamide to prevent disulfide shuffling before the digestion. The proteins were alkylated with iodoacetamide (45 mM) for 1 h at room temperature. In initial experiments, alkylated proteins were precipitated with acetone at neutral pH, dissolved under denaturing conditions in 7 M urea or 6 M GdnHCl (each in 0.4 M  $\text{NH}_4\text{HCO}_3$ ), incubated for 1 h, subsequently diluted 1:10 (urea) or 1:100 (GdnHCl) with water, and digested with trypsin, endoproteinase AspN, or a mixture of trypsin and endoproteinase AspN (enzyme:substrate 1:20 (w/w)) overnight at 37 °C at pH 7.8. The samples were stored at –80 °C prior to mass spectrometric analysis (nano-HPLC/MALDI-TOF/TOF-MS and nano-HPLC/nano-ESI-FTICR-MS). For

laminin  $\beta 1$ , experiments were additionally conducted without precipitation and under nondenaturing conditions using nano-HPLC/nano-ESI-LTQ-Orbitrap mass spectrometry. After alkylation of the protein with iodoacetamide, enzymatic digestion was performed with trypsin (enzyme:substrate 1:16 (w/w)) overnight at 37 °C at pH 7.5. Enzymatic digestion of laminin  $\beta 1$  was also performed under acidic conditions (pH 5.5) using LysN (enzyme:substrate 1:16 (w/w)) overnight at 50 °C. Reactions were stopped with 10% (v/v) TFA solution, and the samples were stored at –80 °C before nano-HPLC/nano-ESI-LTQ-Orbitrap-MS.

The alternative approach, based on a digestion without an alkylation step using pepsin at pH 1.2, prevents a potential rearrangement of SH groups. The laminin fragments were precipitated with acetone (with or without HCl, –80 °C, 30 min), redissolved in HCl (0.084 N, pH 1.2, 25 mM NaCl), and digested with pepsin (1:33 (w/w) enzyme to substrate ratio) for 30 min at 37 °C. The digests were directly analyzed by nano-HPLC/MALDI-TOF/TOFMS.

**Nano-HPLC/MALDI-TOF/TOF Mass Spectrometry.** MALDI-TOF/TOF mass spectrometry was performed on an Ultraflex III instrument (Bruker Daltonik, Bremen, Germany) equipped with a Smart beam laser. Peptide mixtures from enzymatic digests were separated by nano-HPLC (Ultimate 3000; Dionex Corp., Idstein, Germany). Samples were injected by the autosampler (Ultimate 3000; Dionex Corp., Idstein, Germany) and concentrated on a trapping column (PepMap, C18, 300  $\mu\text{m} \times 5 \text{ mm}$ , 3  $\mu\text{m}$ , 100 Å; Dionex, Idstein, Germany) with water containing 0.1% trifluoroacetic acid. After 15 min, the peptides were eluted onto the separation column (PepMap, C18, 75  $\mu\text{m} \times 150 \text{ mm}$ , 3  $\mu\text{m}$ , 100 Å; Dionex, Idstein, Germany), which had been equilibrated with 95% A (A: 5% acetonitrile + 0.05% trifluoroacetic acid). Peptides were separated using the following gradient: 0–30 min, 5–50% B; 30–31 min, 50–95% B; 31–35 min, 95% B (B: 80% acetonitrile + 0.04% trifluoroacetic acid) at flow rates of 300 nL/min and detected by their UV absorptions at 214 and 280 nm. The eluates were fractionated postcolumn (15 s per spot) onto a 384 MTP 800  $\mu\text{m}$  AnchorChip MALDI-target (Bruker Daltonik, Bremen, Germany) using an LC/MALDI fraction collector (ProteinExpert; Bruker Daltonik, Bremen, Germany) controlled via HyStar 3.2.

Positive ionization and reflectron mode were employed for nano-HPLC/MALDI-TOF/TOF-MS measurements of peptide mixtures using  $\alpha$ -cyano-4-hydroxycinnamic acid (HCCA) as matrix. A total of 2000 laser shots per spot were automatically acquired and added to a spectrum in the  $m/z$  range 800–4000. Peptide Calibration Standard II (Bruker Daltonik, Bremen, Germany) was used for external calibration of the mass spectra in the reflectron mode. Data acquisition and data processing were performed using the Flex Control 3.0.101.1 and Flex Analysis 3.0.54 software (Bruker Daltonik, Bremen, Germany). Detected peptide signals with a signal-to-noise ratio of larger than 10 were automatically subjected to MALDI-TOF LID-MS/MS via WarpLC 1.1 (Bruker Daltonik, Bremen, Germany). Additionally, manual MS/MS measurements were conducted from selected peaks of interest.

**Nano-HPLC/Nano-ESI-FTICR Mass Spectrometry.** The peptide mixtures resulting from the *in-gel* digests were separated by reversed-phase C18-RP chromatography on a nano-HPLC system (Ultimate 3000, Dionex; precolumn, PepMap, C18, 300  $\mu\text{m} \times 5 \text{ mm}$ , 3  $\mu\text{m}$ , 100 Å, Dionex; separation column, PepMap, C18, 75  $\mu\text{m} \times 150 \text{ mm}$ , 3  $\mu\text{m}$ , 100 Å, Dionex;

solvent A, 5% acetonitrile and 0.1% formic acid in water; solvent B, 80% acetonitrile and 0.08% formic acid in water) using a gradient from 0 to 60% B in 90 min followed by isocratic elution with 90% B for 3 min. A hybrid LTQ-FT mass spectrometer (Thermo Electron, Bremen, Germany) with a 7 T magnet equipped with a nano-ESI source (Proxeon Biosystems, Odense, Denmark; emitter, distal coated PicoTips, tip i.d. 15  $\mu$ m, New Objective, Woburn, MA) was *online* coupled to the nano-HPLC system. MS data were acquired over 100 min in data-dependent MS<sup>2</sup> mode: Each high-resolution full scan ( $m/z$  300–2000, resolution at  $m/z$  400 was set to 100000) in the ICR cell was followed by 10 product ion scans in the linear trap of the 10 most intense signals in the full-scan mass spectrum (isolation window 3 u). Dynamic exclusion (exclusion duration 20 s, exclusion window  $\pm 5$  ppm) was enabled in order to allow detection of less abundant ions.

**Nano-HPLC/Nano-ESI-LTQ-Orbitrap Mass Spectrometry.** Enzymatic peptide mixtures of laminin  $\beta$ 1 (proteases trypsin and LysN) were additionally analyzed on an Ultimate nano-HPLC system (Dionex Corp.). Samples were desalted and concentrated on a C18 precolumn (Acclaim PepMap, 300  $\mu$ m  $\times$  5 mm, 5  $\mu$ m, 100 Å; Dionex) and separated on a C18 separation column (Acclaim, 75  $\mu$ m  $\times$  250 mm, 3  $\mu$ m, 300 Å; Dionex) using a 40 min linear gradient of 0–50% B (B, 80% ACN, 0.1% formic acid) with a subsequent 15 min washing phase (100% B). The flow rate was set to 300 nL/min. The nano-HPLC system was *online* coupled to an LTQ-OrbitrapXL mass spectrometer (ThermoFisher Scientific, Bremen, Germany) equipped with a nano-ESI source (Proxeon, Odense, Denmark). For LC/MS data acquisition, the software programs Xcalibur 2.0.7 and DCMS-Link 2.0 were employed. One duty cycle comprised one high-resolution mass spectrum ( $m/z$  350–1750,  $R = 60000$ ) in the orbitrap analyzer and fragment ion mass spectra of the three most intense MS signals. Fragmentation methods were CID (collision-induced dissociation) with an analysis of fragment ions in the linear ion trap (LTQ) as well as CID and HCD (higher-energy collision-induced dissociation) with fragment ion analysis in the orbitrap.

**Identification of Disulfides.** Disulfide-linked products were identified using the GPMAW (General Protein Mass Analysis for Windows) software, version 7.01 (Lighthouse Data, Odense, Denmark, [www.gpmaw.com](http://www.gpmaw.com)), Protein Disulfide Linkage Modeler (<http://www.systemsbiochemistry.ca/x-bang/DisulfideModeler/DisulfideModeler.html>), and BioTools 3.1.1.36 (Bruker Daltonik, Bremen, Germany). BioTools and MS2 Assign (<http://roswell.ca.sandia.gov/~mmyoung>) were used for assigning  $m/z$  values of disulfide-linked peptides in fragment ion mass spectra. MS data were searched with mass tolerances of 5 ppm (for LTQ-FT data), 3 ppm (for LTQ-Orbitrap data), and 100 ppm (for Ultraflex III data), whereas for MS/MS data a maximum mass error of 0.8 u (detection of CID-MS/MS fragment ions in the LTQ and MALDI-TOF/TOF-MS/MS data) was allowed.

## RESULTS

**Characterization of Recombinant N-Terminal Laminin  $\beta$ 1 and  $\gamma$ 1 Chain Fragments and the E4 Fragment.** The amino acid sequences of the recombinant N-terminal mouse laminin  $\beta$ 1 and  $\gamma$ 1 chain fragments as well as that of the native E4 fragment, which had been isolated from laminin-111 extracted from EHS tumor tissue (24), were thoroughly analyzed by high-resolution mass spectrometry (Figure 1).

Sequence coverage was found to be 95% (473 of 500 amino acids), 93% (439 of 472 amino acids), and 99% (523 of 527 amino acids) for the recombinant laminin  $\beta$ 1 and  $\gamma$ 1 fragments and the E4 fragment, respectively. The parts of the amino acid sequences, which were not covered by mass spectrometric peptide mass fingerprint (PMF) and peptide fragment fingerprint (PFF) analyses, are likely to comprise regions modified by glycosylation (26).

**Mass Spectrometric Analysis of Disulfides in  $\beta$ -Lactoglobulin.** Analyzing disulfide patterns is not trivial as is outlined in the dispute on the correct disulfide patterns in the N-terminal cysteine-rich somatomedin B (SMB) domain (residues 1–44) of the human glycoprotein vitronectin (27, 28). The use of limited reduction of proteins followed by alkylation of SH groups might cause thiol–disulfide shuffling, which is not easily detected by conventional analytical techniques.

To rule out a potential artifact formation during our analyses, we conducted initial experiments to map the disulfide bonds of bovine  $\beta$ -lactoglobulin.  $\beta$ -Lactoglobulin possesses five cysteines; Cys-66–Cys-160 and Cys-106–119 are connected via disulfide bonds while Cys-121 exhibits a free SH group. We considered  $\beta$ -lactoglobulin to be a suitable model protein to test our various strategies for mapping disulfide bonds. In fact, we observed the correct disulfide bonds and the correct free SH group (Cys-121) for  $\beta$ -lactoglobulin when using trypsin (pH 7.8 and 7.5) or LysN (pH 5.5) as digestion enzymes. With AspN, only very minor signals for alternative disulfide bonds were found with intensities in the mass spectra ca. 1000 times lower than for the peptide signals with correct disulfide bonds. Conclusively, we are certain that our strategies for mapping disulfide bonds do not induce disulfide shuffling.

**Mass Spectrometric Analysis of Disulfides.** First experiments to determine disulfide bond patterns in laminin  $\beta$ 1 and  $\gamma$ 1 fragments were performed using the proteases trypsin and AspN as well as mixtures of both enzymes. As a shuffling of disulfides is prohibited under acidic conditions, we also conducted pepsin digestion at pH 1.2 for the laminin  $\beta$ 1 and  $\gamma$ 1 fragments under investigation. In order to confirm the results found for recombinant laminin  $\beta$ 1 and  $\gamma$ 1 chain fragments, a fragment from tissue-derived laminin, the so-called E4 fragment originating from elastase cleavage of the laminin  $\beta$ 1 chain (24), was analyzed by mass spectrometry in the same fashion using trypsin, AspN, and pepsin as proteolytic enzymes.

All LE domains are thought to possess a (1–3, 2–4, 5–6, 7–8) cysteine connectivity based on the X-ray structure of the laminin  $\gamma$ 1 chain LE domains 7–9, which contain the nidogen-1 binding site (3) (Figure 2A). In contrast, our data from *in-depth* mass spectrometric analyses of both N-terminal laminin  $\beta$ 1 and  $\gamma$ 1 chain fragments (one LN domain plus four LE domains) using trypsin and AspN digests point to a connection of disulfides in a (2–3, 4–5, 6–7, 8–1) arrangement, in which the last cysteine of each LE domain is connected to the first cysteine of the following LE domain (interdomain disulfide, Supporting Information Table S1, Figure 2B).

For the endogenous laminin E4 fragment, several disulfide bonds were found giving the identical linear disulfide pattern (2–3, 4–5, 6–7, 8–1) (Figure 2B) that had already been identified for the recombinant laminin  $\beta$ 1 and  $\gamma$ 1 chain fragments. Using pepsin digestion, the disulfide pattern that had been proposed using trypsin and AspN was confirmed, i.e., the Cys connections 6–7 in LE domain 1, 6–7 in LE domain 2, 4–5 in LE domain 3, and 2–3 in LE domain 4 of laminin  $\beta$ 1, Cys connections 4–5 in LE domain 1, 6–7 in LE domain 3, and 6–7

(A) Laminin $\beta$ 1:	
1	APLVQEPEFS YGCAEGSCYP ATGDLLIGRA QKLSVTSTCG LHKPEPYCIV
51	SHLQEDKKCF ICDSDPYHE TLNPDShLIE NVVTTTFAPNR <b>LKIWWQSENG</b>
101	<b>VENVTIQ</b> LDL EAEFHFTHLI MTFKTFRPAA MLIERSSDFG KTWGVYRYFA
151	YDCESSFPGI STGPMKKVDD <b>IICDS</b> RYSDI EPSTEGEVIF RALDPAFKIE
201	DPYSPRIQNL LKITNLRIKF VKLHTLGDNL LDSRMEIREK YYYAVYDMVV
251	RGN <b>FCY</b> GHA <b>SECAP</b> VDGVN EEVEGMVHGH <b>CMCR</b> HNTKGL <b>NCEL</b> CMDFYH
301	DLPWRPAEGR NSNA <b>CKK</b> CNC NEHSSSCHFD MAVFLATGNV <b>SGGV</b> CDNCQH
351	NTMGRNCEQC KPFYFQHPER <b>DIR</b> DPNLCEP <b>CTCD</b> PAGSEN GGI <b>CD</b> GYTDF
401	SVGLIAGQ <b>CR</b> <b>CKLH</b> VEGERC DVCKEGFYDL SAEDPYG <b>CKS</b> CACNPLGTIP
451	GGN <b>PCD</b> SETG <b>YCY</b> CKRLVTG <b>QRCD</b> QCLPQH WGLSNDLDGC RAAAHHHHHH
(B) Laminin $\gamma$ 1:	
1	APLVHHHHHH ALVAMDECAD EGGRPQRCMP EFVNAA <b>FNVT</b> VVATNTCGTP
51	PEEYCVQ <b>TGV</b> TGVTKSCHLC DAGQQHLQHG AAFLTDYNNQ ADTTWWQSQT
101	MLAGVQYPNS <b>INLTL</b> HLGKA FDITYVRLKF HTSRPESFAI YKRTREDGPW
151	IPYQYYSGSC ENTYSKANRG FIRTGGDEQQ ALCTDEFSDI SPLTGGNVAF
201	STLEGRPSAY NFDNSPVLQE WVTATDIRVT LNRLNTFGDD VFNEPKVLKS
251	YYYAISDFAV GGR <b>CKC</b> NGHA <b>SECV</b> KNEFDK <b>LMCN</b> CKHNTY GVD <b>CEK</b> CLPF
301	FNDRPWRRAT AESASESLPC <b>D</b> CNGRSQ <b>ECY</b> FDPELYRSTG HGGH <b>CTN</b> ORD
351	NTDGAK <b>CERC</b> RENFFR <b>LGNT</b> <b>EAC</b> SPCHCSP VGSLSTQ <b>CD</b> S YGRCS <b>CK</b> PGV
401	MGDK <b>CDRC</b> QP GFHSLTEAGC <b>RPC</b> SCDPSGS TDECNVETGR <b>CVCK</b> DNVEGF
451	<b>NCER</b> CKPGFF NLESSNPK <b>GC</b> <b>TF</b>
(C) Native Laminin Fragment EHS-E4:	
1	qEPEFSYGCA EGSCYPATGD LLIGRAQKLS VTSTCGLHKP EPYCIVSHLQ
51	EDKKCFICDS RDPYHETLNP DSHLIENVVT TFAPNRL <b>KIW</b> <b>WQSENG</b> <b>VENV</b>
101	<b>TIQ</b> LDLEAEF HFTHLIMTFK TFRPAAMLIE RSSDFG <b>KTWG</b> VYRYFAYDCE
151	SSFPGISTGP MKKVDDIICD SRYSDIEPST EGEVIFRALD PAFKIEDPYS
201	PRIQNLLKIT NLRKFVKLH TLGDNLLDSR MEIREKYYA VYDMVVRGN <b>C</b>
251	<b>FCY</b> GHASE <b>CA</b> PVDGVNEEVE GMVHGH <b>CMCR</b> HNTKGLN <b>CEL</b> CMDFYHDLPW
301	RPAEGRNSNA <b>CKKCN</b> NEHS SSCHFDMAVF LATGNVSGGV <b>CDNC</b> QHNTMG
351	RNCEQ <b>CK</b> KPFY FQHPERDIRD PNLCEP <b>CTCD</b> PAGSENGG <b>IC</b> DGYTDFSVGL
401	IAGQ <b>CR</b> CKLH VEGERC <b>CDVCK</b> EGFYDLSAED PYGCK <b>SCACN</b> PLGTIPGGNP
451	<b>CD</b> SETGYCYC KRLVTG <b>QRCD</b> <b>QCLP</b> QHWGLS NDLDG <b>CRPCD</b> <b>CDLGGALNNS</b>
501	<b>CSEDSGQCSC</b> LPHMIGRQCN EVESGYV

FIGURE 1: Amino acid sequences of (A) recombinant N-terminal laminin  $\beta$ 1 chain fragment (one LN plus four LE domains), (B) recombinant N-terminal laminin  $\gamma$ 1 chain fragment (one LN plus four LE domains), and (C) the native E4 fragment. Laminin LE domains are shown in gray; cysteines are printed in white. Amino acids that were detected during peptide mass fingerprint and peptide fragment fingerprint analyses are shown in bold. The putative glycosylation sites are underlined. The N-terminal amino acid of the native E4 fragment was found to be pyroglutamate.

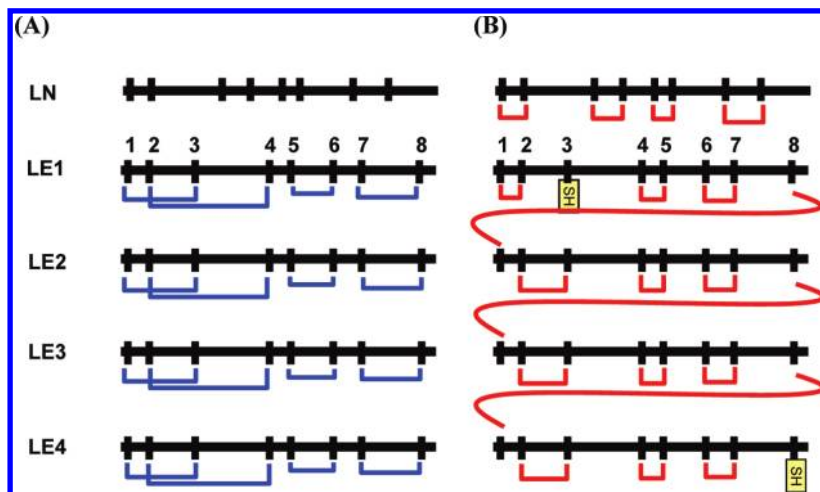


FIGURE 2: Disulfide bond patterns of laminin LE domains. The cysteines are numbered and indicated as black bars. (A) Disulfide pattern in LE domains 7–9 from the laminin  $\gamma$ 1 chain (3). (B) Disulfide pattern detected in the recombinant N-terminal laminin  $\beta$ 1 and  $\gamma$ 1 fragments and in the E4 fragment used in this study. LE domains 7–9 from the laminin  $\gamma$ 1 chain had been found to possess a (1–3, 2–4, 5–6, 7–8) connectivity. In contrast, our data from *in-depth* mass spectrometric analyses of both recombinant N-terminal laminin  $\beta$ 1 and  $\gamma$ 1 chain fragments and the laminin E4 fragment point to a linear connection of disulfides in a (2–3, 4–5, 6–7, 8–1) arrangement.

in LE domain 4 of laminin  $\gamma$ 1, as well as Cys connections 4–5 in LE domain 1 and 6–7 in LE domain 2 of E4 fragment (Supporting Information Table S2).

The disulfides recognized in the recombinant and proteolytically produced laminin fragments using different mass spectrometric techniques and different digestion procedures are summarized in Supporting Information Tables S1 and S2.

**Mass Spectrometric Analysis of Disulfides of Laminin  $\beta$ 1 Using Trypsin and LysN.** For laminin  $\beta$ 1, mapping of disulfide bonds was additionally conducted under nonreducing conditions using exclusively electrospray ionization mass spectrometry. By this, we aimed to address potential concerns that disulfide shuffling might be induced during the MALDI process.

Using trypsin (pH 7.5) as digestion enzyme, seven disulfides and one free cysteine were identified (Supporting Information Table S3) whereas with LysN (at pH 5.5 where a potential disulfide shuffling is prohibited) merely four disulfide bonds were found during five repetitive experiments. The fact that only seven and four disulfide bonds, respectively, were identified is attributed to the experimental conditions, in which the protein was neither reduced nor subjected to denaturing conditions at any point of the analysis. Thus, the protein remains folded, resulting in an increased resistance to proteases and a lower sequence coverage. Yet, the disulfide bonds detected herein confirmed the results of a linear disulfide pattern in N-terminal laminin LN and LE domains (Supporting Information Table S3).

**Disulfide Bond Patterns.** The third cysteine of laminin  $\beta$ 1 and  $\gamma$ 1 chain fragment LE1 domains (Cys-263, -259, and -273 in the recombinant laminin  $\beta$ 1 and  $\gamma$ 1 chain fragments and the E4 fragment, respectively) was found to be present as a free SH group (Figure 2B, Supporting Information Table S1). For the last three cysteines of the laminin  $\gamma$ 1 chain fragment (Cys-452, Cys-455, and Cys-470), two possible disulfide bonds were detected, pointing to a 6–8 (Cys-452 to Cys-470) and to a 7–8 (Cys-455 to Cys-470) connection of cysteines. This finding is not surprising as these amino acids do not represent the natural C-terminus but are an “artificial” C-terminus of the laminin  $\gamma$ 1 chain fragment. Based on the disulfide patterns of the preceding LE domains, a connection of Cys-470 to the following cysteine residue can be assumed in native laminin.

As examples, mass spectrometric analysis of amino acid sequence 352–366 of laminin fragment E4 (precursor ion  $[M + H]^+$  at  $m/z$  1923.826) is presented in Figure 3A, confirming the disulfide bond between Cys-353 (corresponding to Cys-6 in LE domain 2) and Cys-356 (Cys-7 in LE domain 2), while MS/MS analysis of amino acids 311–329 of laminin  $\beta$ 1 (precursor ion  $[M + H]^+$  at  $m/z$  2108.723) identified the disulfide bonds between Cys-315 (Cys-8 in LE domain 1) and Cys-318 (Cys-1 in LE domain 2) as well as between Cys-320 (Cys-2 in LE domain 2) and Cys-327 (Cys-3 in LE domain 2) (Figure 3B).

Intriguingly, a number of cysteines (Supporting Information Table S4) were detected both as disulfide bonds and as free SH groups, suggesting that cysteines in laminins are present in both their oxidized and reduced forms. Therefore, an alkylation step was performed when digestion with trypsin and/or endoprotease AspN was employed in order to prevent a rearrangement of SH groups at pH 7.8. It is known that extracellular matrix proteins are heterogeneous species, in which cysteines are only partially oxidized. For example, the native hexameric NC1 domain of collagen IV contains 4–11% free sulfhydryl groups, depending on preparation and source (29). Similarly, thrombospondin-1 subunits always carry one sulfhydryl group which does, however, vary its position between 12 different cysteine residues, with each of these carrying a free thiol in only a small fraction of thrombospondin-1 molecules (30). During our detailed mass spectrometry-based analysis of disulfide patterns in laminin LE domains, we never observed an alternative disulfide pattern compared to the linear pattern described herein, neither using trypsin, nor AspN, nor LysN, nor pepsin as digestion enzymes. Moreover, the new disulfide pattern was observed for the recombinant fragments of the laminin  $\beta$ 1 and  $\gamma$ 1 chains as well as for the E4 fragment that was derived from laminin-111 extracted from EHS tumor tissue.

## DISCUSSION

Biological results obtained with EGF and some EGF-like domains have shown that disulfide isomers possess significant bioactivity suggesting that the EGF fold can accommodate alternate disulfide-bonding patterns (31–33). Disulfide bonds in murine EGF have been altered to produce seven different

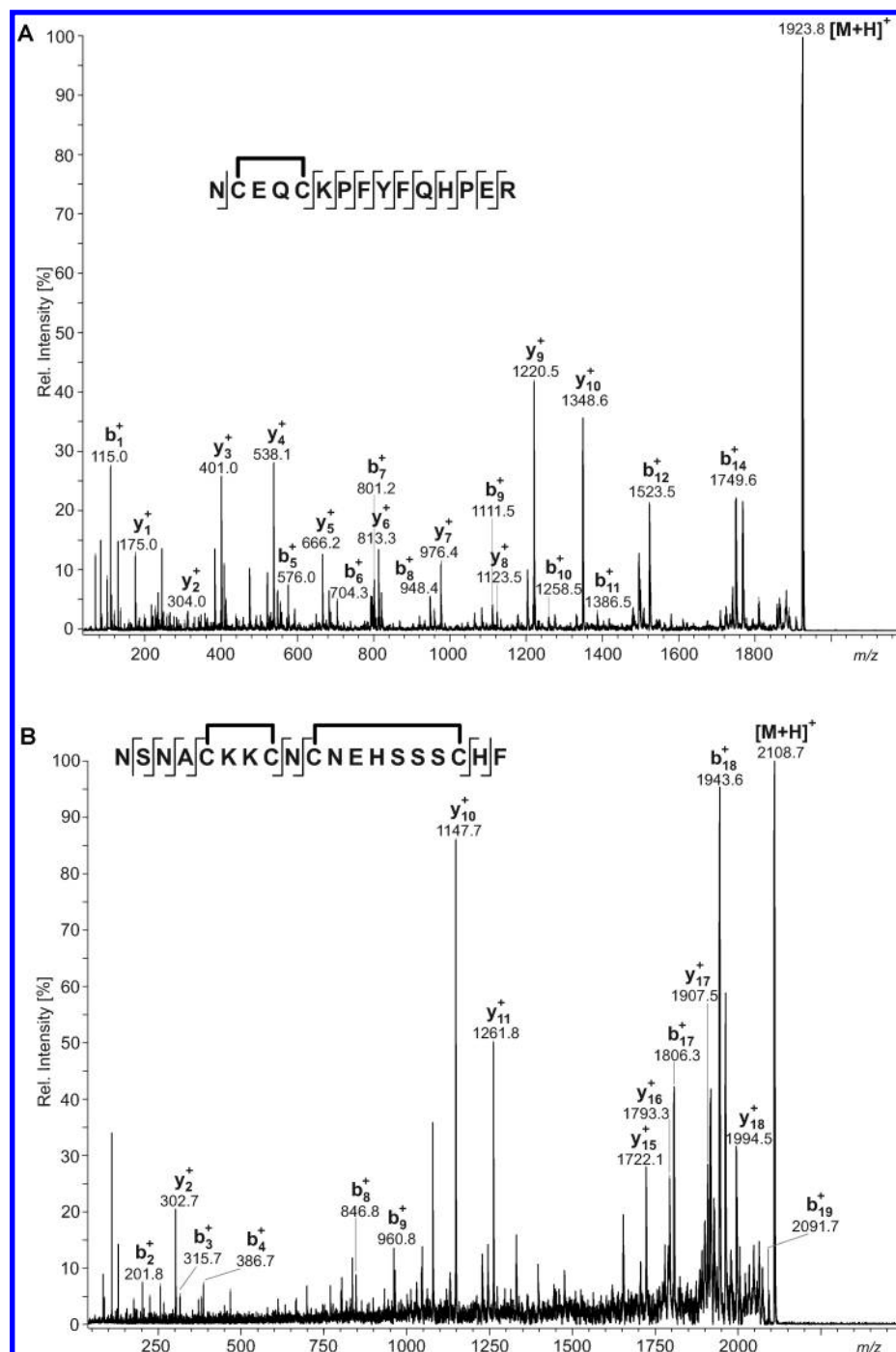


FIGURE 3: (A) Mass spectrometric analyses (MALDI-TOF/TOF-MS/MS) of amino acids 352–366 of the native laminin fragment E4. The fragment ion mass spectrum of the precursor ion  $[M + H]^+$  at  $m/z$  1923.826 confirms the disulfide bond between Cys-353 and Cys-356. (B) Mass spectrometric analyses (MALDI-TOF/TOF-MS/MS) of amino acids 311–329 of the recombinant N-terminal laminin  $\beta$ 1 fragment. The fragment ion mass spectrum of the precursor ion  $[M + H]^+$  at  $m/z$  2108.723 confirms the disulfide bonds between Cys-315 and Cys-318 and between Cys-320 and Cys-327 (see also Supporting Information Table S1).

patterns, and the resulting structures were calculated incorporating all the restraints from the highest resolution restraint set available (34). Most interestingly, this showed that two other disulfide bond patterns, namely, (1–2, 3–4, 5–6) and (1–3, 2–5, 4–6), satisfied the restraints as well as the native (1–3, 2–4, 5–6) disulfide pattern (32). In fact, the results on the basis of distance and dihedral violations were indistinguishable from the native disulfide bond pattern. For all seven isomers, the final calculated structures were highly similar to the structure of native EGF (rmsd of all atoms between 1.5 and 2 Å). The observation that several different disulfide bond patterns can be satisfied by the

EGF backbone fold suggests that disulfide bonding does not play a crucial role in establishing the EGF fold.

The conformational stability of human EGF and the structures of denatured EGF have been investigated recently (35). Using different denaturing conditions, the three native disulfide bonds (1–3, 2–4, 5–6) in native EGF reshuffle, creating a highly heterogeneous mixture of various disulfide-scrambled isomers. Under heat denaturation, the most predominant isomer was that exhibiting a linear connectivity of cysteines (1–2, 3–4, 5–6) (35).

The novel disulfide pattern described herein has not been reported for LE domains so far. In our experiments, we did not

observe a mixture of different disulfide patterns, suggesting that the pattern reported herein for the N-terminal laminin LE domains is not caused by denaturation of the protein. This is also confirmed by the fact that we did not find any aggregate formation of the laminin fragments used for the present study when SDS–PAGE analysis was performed after purification of the proteins (data not shown). If disulfide interchange had occurred, interchain disulfide bond formation with the subsequent formation of high-molecular-weight laminin aggregates could be expected to take place.

It is not unique that a protein exhibits varying disulfide patterns in its EGF domains. For instance, the fifth EGF-like domain in thrombomodulin, the high-affinity binding site for thrombin, exhibits a (1–2, 3–4, 5–6) disulfide pattern in contrast to the fourth EGF domain, which has a classical (1–3, 2–4, 5–6) structure (31, 33). Indeed, when the fifth EGF-like domain in thrombomodulin was synthesized in a classical (1–3, 2–4, 5–6) disulfide pattern by differential protection methods, it showed a far lower binding affinity for thrombin (31). An isomer of the EGF-like domain of bovine TGF- $\alpha$  with the disulfide bonding (1–4, 2–3, 5–6) has also been shown to exhibit bioactivity, albeit lower than that of native TGF- $\alpha$  with the disulfide pattern (1–3, 2–4, 5–6) (36).

An interesting observation was made in the present study as we do not find the crossed disulfide pattern described for the laminin  $\gamma$ 1 chain LE domains 7–9 (3). This was caused by difficulties in enzymatic digestion of LE domains 7–9 resulting in mass spectra that were impossible to interpret. It should be stressed that the laminin  $\gamma$ 1 chain LE domains 7–9 had been isolated under identical conditions as the laminin fragments used for the present studies. This hints that the disulfide bonds in LE domains 7–9 are indeed different from these in LE domains 1–4. The LN domains and the following LE domains 1–4 are important for laminin self-interaction, which occurs through the laminin short arms, whereas LE domain 8 harbors the nidogen binding site. Based on the X-ray structure of LE domains 7–9 (3) it had been assumed that all laminin LE modules exhibit identical disulfide connections. Our results show that this is not the case and raises the possibility that other LE domains may also show varying disulfide arrangements.

The thiol–disulfide redox exchange mechanism for cleaving disulfide bonds in the extracellular milieu suggests that disulfide bonds may be cleaved in mature proteins, having an impact on protein function (37, 38). Cleavage of disulfide bonds might often be reversible with the balance between disulfide-bonded and cleaved forms being a requirement for the respective protein's function.

The observed interdomain disulfide bonds in the LE domains may also play some role in folding of the protein as we have found only very low recombinant expression of N-terminal laminin chain fragments containing either one or two LE domains (8). Presumably these constructs are unstable due to misfolding and are degraded by intracellular quality control mechanisms. The longer, recombinantly expressed laminin fragments are secreted and biologically functional (8).

Versatility in disulfide bonding may provide a tool in evolution to provide variable structures from relatively conserved protein domains. The fact that the first two disulfide constrained loops are free from the usual EGF knot induced by the crossing of disulfides presumably gives this region and each LE module a greater freedom in its structure. This may have functional relevance as it would allow the interconnecting laminin short

arms to be more flexible. This may be important as three LN domains are believed to interact in a binding unit and the binding surfaces themselves may therefore be under strong positional constraints.

We conclude that laminin LE domains possess variable arrangements of disulfides, which are important for exerting their specific functions.

## ACKNOWLEDGMENT

The authors are indebted to Karl Mechtler and Christoph Stingl (IMP Vienna) for conducting initial nano-HPLC/nano-LTQ-FT-MS measurements and to Dr. Hauke Lilie for valuable discussions.

## SUPPORTING INFORMATION AVAILABLE

A summary of disulfide bonds and free SH groups in recombinant N-terminal laminin  $\beta$ 1 and  $\gamma$ 1 chain fragments and the native E4 fragment (Tables S1–S4). This material is available free of charge via the Internet at <http://pubs.acs.org>.

## REFERENCES

- Wouters, M. A., Rigoutsos, I., Chu, C. K., Feng, L. L., Sparrow, D. B., and Dunwoodie, S. L. (2005) Evolution of distinct EGF domains with specific functions. *Protein Sci.* 14, 1091–1103.
- Bersch, B., Hernandez, J. F., Marion, D., and Arlaud, G. J. (1998) Solution structure of the epidermal growth factor (EGF)-like module of human complement protease C1r, an atypical member of the EGF family. *Biochemistry* 37, 1204–1214.
- Stetefeld, J., Mayer, U., Timpl, R., and Huber, R. (1996) Crystal structure of three consecutive laminin-type epidermal growth factor-like (LE) modules of laminin  $\gamma$ 1 chain harboring the nidogen binding site. *J. Mol. Biol.* 257, 644–657.
- Xiong, J. P., Stehle, T., Diefenbach, B., Zhang, R., Dunker, R., Scott, D. L., Joachimiak, A., Goodman, S. L., and Arnaout, M. A. (2001) Crystal structure of the extracellular segment of integrin  $\alpha$ V $\beta$ 3. *Science* 294, 339–345.
- Beglova, N., Blacklow, S. C., Takagi, J., and Springer, T. A. (2002) Cysteine-rich module structure reveals a fulcrum for integrin rearrangement upon activation. *Nat. Struct. Biol.* 9, 282–287.
- Burgeson, R. E., Chiquet, M., Deutzmann, R., Ekblom, P., Engel, J., Kleinman, H., Martin, G. R., Meneguzzi, G., Paulsson, M., Sanes, J., Timpl, R., Tryggvason, K., Yamada, Y., and Yurchenco, P. D. (1994) A new nomenclature for the laminins. *Matrix Biol.* 14, 209–211.
- Aumailley, M., Bruckner-Tuderman, L., Carter, W. G., Deutzmann, R., Edgar, D., Ekblom, P., Engel, J., Engvall, E., Hohenester, E., Jones, J. C. R., Kleinmann, H. K., Marinkovich, M. P., Martin, G. R., Mayer, U., Meneguzzi, G., Miner, J. H., Miyazaki, K., Patarroyo, M., Paulsson, M., Quaranta, V., Sanes, J. R., Sasaki, T., Sekiguchi, K., Sorokin, L. M., Talts, J. F., Tryggvason, K., Uitto, J., Virtanen, I., von der Mark, K., Wewer, U. M., Yamada, Y., and Yurchenco, P. D. (2005) A simplified laminin nomenclature. *Matrix Biol.* 24, 326–332.
- Odenthal, U., Haehn, S., Tunggal, P., Merkl, B., Schomburg, D., Frie, C., Paulsson, M., and Smyth, N. (2004) Molecular analysis of laminin N-terminal domains mediating self-interactions. *J. Biol. Chem.* 279, 44504–44512.
- Yurchenco, P. D., Tsilibary, E. C., Charonis, A. S., and Furthmayr, H. (1985) Laminin polymerization in vitro. Evidence for a two-step assembly with domain specificity. *J. Biol. Chem.* 260, 7636–7644.
- Nielsen, P. K., and Yamada, Y. (2001) Identification of cell-binding sites on the laminin  $\alpha$ 5 N-terminal domain by site directed mutagenesis. *J. Biol. Chem.* 276, 10906–10912.
- Sasaki, M., Kato, S., Kohno, K., Kartin, G. R., and Yamada, Y. (1987) Sequence of cDNA encoding the laminin B1 chain reveals a multidomain protein containing cysteine-rich repeats. *Proc. Natl. Acad. Sci. U.S.A.* 84, 935–939.
- Sasaki, M., Kleinmann, H. K., Huber, H., Deutzmann, R., and Yamada, Y. (1988) Laminin, a multimodule protein: the A chain has a unique globular domain and homology with the basement proteoglycan and the laminin B chains. *J. Biol. Chem.* 263, 16536–16544.
- Sasaki, M., and Yamada, Y. (1987) Structure of the laminin B2 chain shows multimodule structures homologous to the  $\beta$ 1 chain. *J. Biol. Chem.* 262, 17111–17117.

14. Beck, K., Hunter, I., and Engel, J. (1990) Structure and function of laminin: anatomy of a multidomain glycoprotein. *FASEB J.* 4, 148–160.
15. Timpl, R., and Brown, J. C. (1996) Supramolecular assembly of basement membranes. *BioEssays* 18, 123–132.
16. Timpl, R. (1993) Proteoglycans of basement membranes. *Experientia* 49, 417–428.
17. McMahan, U. J., Horton, S. E., Werle, M. J., Honig, L. S., Kröger, S., Ruegg, M. A., and Escher, G. (1992) Agrin isoforms and their role in synaptogenesis. *Curr. Opin. Cell Biol.* 4, 869–874.
18. Cirulli, V., and Yebra, M. (2007) Netrins: beyond the brain. *Nat. Rev. Cell Biol.* 8, 296–306.
19. Weston, M. D., Eudy, J. D., Fujita, S., Yao, S., Usami, S., Cremers, C., Greenberg, J., Ramesar, R., Martinin, A., Moller, C., Smith, R. J., Sumegi, J., and Kimberling, W. J. (2000) Genomic structure and identification of novel mutations in usherin, the gene responsible for Usher syndrome type IIa. *Am. J. Hum. Genet.* 66, 1199–1210.
20. Pöschl, E., Mayer, U., Stetefeld, J., Baumgartner, R., Holak, T. A., Huber, R., and Timpl, R. (1996) Site-directed mutagenesis and structural interpretation of the nidogen binding site of the laminin  $\gamma$ 1 chain. *EMBO J.* 15, 5154–5159.
21. Panayatou, G., End, P., Aumailley, M., Timpl, R., and Engel, J. (1989) Domains of laminin with growth-factor activity. *Cell* 56, 93–101.
22. Kalkhof, S., Haehn, S., Ihling, C., Smyth, N., and Sinz, A. (2008) Determination of disulfide bond patterns in laminin  $\beta$ 1 chain N-terminal domains by nano-high performance liquid chromatography/matrix-assisted laser desorption/ionization time-of-flight/time-of-flight mass spectrometry. *Rapid Commun. Mass Spectrom.* 22, 1933–1940.
23. Paulsson, M., Aumailley, M., Deutzmann, R., Timpl, R., Beck, K., and Engel, J. (1987) Laminin-nidogen complex: extraction with chelating agents and structural characterization. *Eur. J. Biochem.* 166, 11–16.
24. Ott, U., Odermatt, E., Engel, J., Furthmayr, H., and Timpl, R. (1982) Protease resistance and conformation of laminin. *Eur. J. Biochem.* 123, 63–72.
25. Schulz, D. M., Ihling, C., Clore, G. M., and Sinz, A. (2004) Mapping the topology and determination of a low-resolution three-dimensional structure of the calmodulin-melittin complex by chemical cross-linking and high resolution FTICRMS: direct demonstration of multiple binding modes. *Biochemistry* 43, 4703–4715.
26. Fujiwara, S., Shinkai, H., Deutzmann, R., Paulsson, M., and Timpl, R. (1988) Structure and distribution of N-linked oligosaccharide chains on various domains of mouse tumour laminin. *Biochem. J.* 252, 453–461.
27. Kamikubo, Y., De Guzman, R., Kroon, G., Curriden, S., Neels, J. G., Churchill, M. J., Dawson, P., Oldziej, S., Jagielska, A., Scheraga, H. A., Loskutoff, D. J., and Dyson, H. J. (2004) Disulfide bonding arrangements in active forms of the somatomedin B domain of human vitronectin. *Biochemistry* 43, 6519–6534.
28. Zhou, A. (2007) Functional structure of the somatomedin B domain of vitronectin. *Protein Sci.* 16, 1502–1508.
29. Weber, S., Dölz, R., Timpl, R., Fessler, J. H., and Engel, J. (1988) Reductive cleavage and reformation of the interchain and intrachain disulphide bonds in the globular hexameric domain NC1 involved in network assembly of basement membrane collagen (type IV). *Eur. J. Biochem.* 175, 229–236.
30. Speziale, M. V., and Detwiler, T. C. (1990) Free thiols of platelet thrombospondin. Evidence for disulphide isomerization. *J. Biol. Chem.* 265, 17859–17867.
31. Sampoli Benitez, B. A., Hunter, M. J., Meininger, D. P., and Komives, E. A. (1997) Structure of the fifth EGF-like domain of thrombospondin: an EGF-like domain with a novel disulfide-bonding pattern. *J. Mol. Biol.* 273, 913–926.
32. Sampoli Benitez, B. A., and Komives, E. A. (2000) Disulfide bond plasticity in epidermal growth factor. *Proteins* 40, 168–174.
33. White, C. E., Hunter, M. J., Meininger, D. P., Garrod, S., and Komives, E. A. (1996) The fifth EGF-like domain of thrombospondin does not have an EGF-like disulfide pattern. *Proc. Natl. Acad. Sci. U.S.A.* 93, 10177–10182.
34. Tejero, R., Bassolino-Klimas, D., Bruccoleri, R. E., and Montelione, G. T. (1996) Simulated annealing with restrained molecular dynamics using CONGEN: energy refinement of the NMR solution structures of epidermal and type-alpha transforming growth factors. *Protein Sci.* 5, 578–592.
35. Chang, J. Y., and Li, L. (2002) The disulfide structure of denatured epidermal growth factor: preparation of scrambled disulfide isomers. *J. Protein Chem.* 21, 203–213.
36. Tou, J. S., McGrath, M. F., Zupiec, M. E., Byatt, J. C., Violand, B. N., Kaempfe, L. A., and Vineyard, B. D. (1990) Chemical synthesis of bovine transforming growth factor- $\alpha$ : synthesis, characterization and biological activity. *Biochem. Biophys. Res. Commun.* 167, 484–491.
37. Chen, V. M., and Hogg, P. J. (2006) Allosteric disulfide bonds in thrombosis and thrombolysis. *J. Thromb. Haemostasis* 4, 2533–2541.
38. Hogg, P. J. (2003) Disulfide bonds as switches for protein function. *Trends Biochem. Sci.* 28, 210–214.